Morphology and dynamic mechanical properties of AB crosslinked polymers based on polyurethanes

Liu Jingjiang, Liu Wenzhong, Zhou Huarong, Hou Chunrong and Ni Shaoru

Changchun Institute of Applied Chemistry, Academia Sinica, Changchun, Jilin, People's Republic of China

(Received 6 March 1989; accepted 26 November 1990)

Polyoxypropylene glycol (PPG) (or castor oil) and toluene diisocyanate (TDI) were mixed, and the prepolymer polyurethane (PU) (I) was formed. Vinyl-terminated polyurethane (II) was prepared from (I), and hydroxyethyl acrylate, AB crosslinked polymers (ABCPs) were synthesized from (II) and vinyl monomers such as styrene, methyl methacrylate, vinyl acetate, etc. The dynamic mechanical properties and morphology of ABCPs were measured. The ABCPs based on PPG have double glass transition temperatures (T_g) on the tan δ vs. temperature curves. They display a two-phase morphology with plastic components forming the continuous phase and PU-rich domains forming the separated phase on the electron micrographs. Irregular shapes and a highly polydisperse distribution of PU-rich domain sizes were observed. The crosslink density of ABCPs has a notable effect on the morphology and properties. The average diameter of the PU-rich domains depends on the molecular weight of prepolymer PPG. The highly crosslinked structures will produce large numbers of very small domains. ABCPs based on castor oil show a single T_g relaxation on the dynamic mechanical spectra. The compatibility between the two components is much better in ABCPs based on castor oil than in those based on PPG, because there is a high crosslink density in the former. Comparison of the dynamic mechanical spectra of ABCP and interpenetrating networks (IPN) based on castor oil with similar crosslink density and composition imply that the two components in ABCP are compatible whereas microphase separation occurs in IPN. An improvement in the compatibility is achieved by the crosslinking between the two networks.

(Keywords: morphology; dynamic mechanical properties; crosslinked polymers; polyurethanes)

INTRODUCTION

The term AB crosslinked polymers (ABCPs) or joined interpenetrating polymer network (IPN) refers to polymers in which polymer A is bonded to polymer B at both ends or at various points along the chains. Thus, ideally, one network is generated for ABCP compared to two different networks ideally synthesized for IPNs. In ABCPs, while polymer A is bonded primarily to polymer B, it is not crosslinked to itself. Ideal IPNs are unique blends of two crosslinked polymers containing essentially no covalent bonds or grafts between networks. Both ABCPs and IPNs are thermoset combinations of polymers.

Soluble and thermoplastic polymer materials prepared from more than one type of monomer units in which monomer units are attached in long sequences include blends of homopolymers, certain types of copolymer and their blends with one or more homopolymers. Examples of the simplest and most relevant copolymer species in this category and based on two monomers A and B are linear AB and ABA block copolymers and non-linear block polymer of A_2B. In order to distinguish the bonding type in ABCPs from the case where the product remains thermoplastic, we designated it conterminous linking[1].

Bamford and Eastmond[2–4] described a general method of preparing ABCPs of known structure by reacting a preformed polymer (the A component) having reactive halogen in side-chains with a metal carbonyl in the presence of a monomer. The metal carbonyl specifically removes halogen atoms from the preformed polymer to produce radical sites on the side-groups of the A chains. These macroradicals initiate polymerization of the monomer to produce growing chains of polymer B attached to the A chains. Combination termination of the propagating grafts produces B crosslinks, while disproportionation termination generates B branches on A chains. The specificity of the initiating system ensures that, in the absence of chain transfer, no homopolymer of B is formed.

In another case of preparing ABCPs, a precursor polymer A with reactive functions, such as organometallic sites, alcohol functions, vinyl or hydrosilane groups, at both ends is coupled with a multifunctional polymer B. Although ABCPs have been investigated and reviewed during the past 20 years, by some authors[5–8], the details of morphology and properties are still incompletely known.

In this paper we report on the synthesis, morphology and dynamic mechanical properties of a series of ABCPs based on vinyl-terminated polyurethane (VTPU) and vinyl monomers.

These ABCP, or joined IPN, materials exhibited high damping over a broad temperature range for controlling vibration and noise. Some thermoplastics may exhibit excellent mechanical damping properties as ABCPs, but they will flow when the temperature is higher than their

0032-3861/91/081361-08

T_g. The polymer sheets will be softened and stripped from metal plates, so that they cannot be used in engineering. ABCPs can overcome this disadvantage. This is another reason why we selected ABCPs for controlling noise and damping vibration.

EXPERIMENTAL

Materials

All the reagents used are listed in *Table 1*. The commercial reagents were purified before use. When necessary, functional and other analyses were carried out to check the indications given by the manufacturers.

Synthesis

Polyurethane. A standard synthesis proceeds as follows. The calculated amounts of polyoxypropylene glycol (PPG) and toluene diisocyanate (TDI) (–NCO/–OH = 2) were mixed and stirred thoroughly in a dry nitrogen atmosphere for a few minutes and degassed under vacuum at 80°C for 15 to 20 min. Polyurethane (PU) (I) was synthesized:

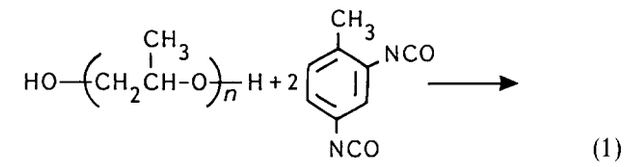

(1)

Vinyl-terminated polyurethane (VTPU). PU (I) was mixed with hydroxyethyl acrylate (HEA) (–OH/–NCO = 1.1) and catalysts by stirring at 60°C for 15 to 20 min. VTPU (II) was formed as follows:

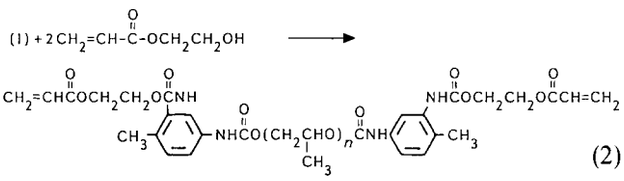

(2)

AB crosslinked polymers. Preparation of all the various ABCPs that will be discussed in this paper followed the same basic procedure. Calculated amounts of VTPU prepolymer (II), vinyl monomers (such as styrene, methyl methacrylate, vinyl acetate) and initiator were mixed and stirred at 30°C. Radical copolymerization of the VTPU (II) and vinyl monomers is initiated. After a few minutes, the blend is poured into a glass mould. The ABCPs (III) were formed at room temperature for 24 h.

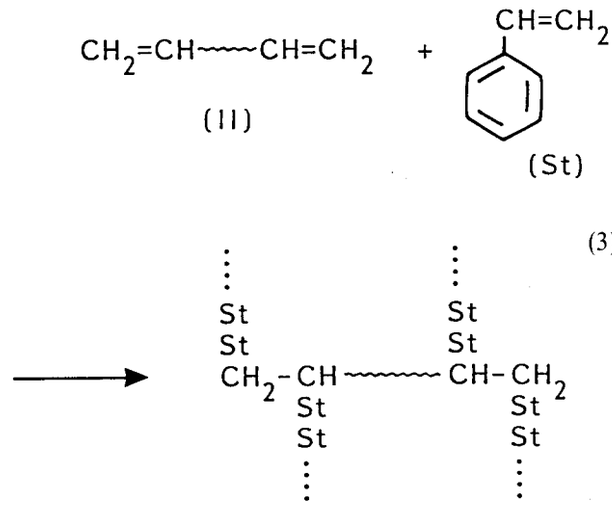

(3)

The resulting sheets were placed in a vacuum over (100°C) for at least 24 h to remove residual monomers. The weight loss during this period was always less than 3%. When we use castor oil instead of PPG, another series of ABCPs based on castor oil PU were obtained.

Table 1 Materials

Material code	Description
PPG	Polyoxypropylene glycol ($\bar{M}_n$ = 1570, 1510 and 900; 1.104 OH/kg; density 1.0 g ml^{-1})
CO	Castor oil
TDI	Toluene diisocyanate
HEA	Hydroxyethyl acrylate (stabilizer: hydroquinone 0.5%)
Vinyl monomers	
St	Styrene
MMA	Methyl methacrylate
VAc	Vinyl acetate
BMA	Butyl methacrylate
	etc.

Dynamic mechanical spectroscopy

Strips ($20 \times 4 \times 0.5$ mm^3) of each material were examined in a Rheovibron Dynamic Viscoelastometer model DDV-II-EA in the tensile mode over a temperature range of about −75 to 150°C at a heating rate of 2°C min^{-1} and a strain amplitude of 0.02%. The complex modulus E^*, storage modulus E', loss modulus E'' and loss factor tan δ were measured. The temperature at which the loss tangent is a maximum was taken as the dynamic glass transition temperature T_g. It happens that the viscosity of some test samples decreases too rapidly at high temperature that dynamic mechanical spectroscopy cannot be carried out. In the figures each point represents a single sample. Overall experimental error is suggested by the deviation of the data from the smooth curves shown. Replicate runs with strips from a given sample indicated that while the tan δ curves were highly reproducible, absolute values of E' may vary by as much as 20%.

Solvent extraction

ABCPs (0.5 mm thick) were solvent-extracted in a Soxhlet apparatus with benzene. The refluxing was stopped when no soluble parts were released. The amount of extract was determined and analysed by i.r. spectroscopy.

Electron micrograph measurements

Samples of ABCPs were stained in osmium tetroxide for 2 weeks following Kato's staining techniques[9], after which they were embedded in epoxy resin. The specimens were cut to thicknesses of about 0.1 μm. Electron micrographs were taken by direct observation of the ultra-thin sections. Samples were prepared for scanning

electron microscopy (SEM) by freeze-fracturing in liquid nitrogen and applying a gold coating of approximately 200 Å. Micrographs were obtained using a scanning electron microscope model SEM JXA-840.

RESULTS AND DISCUSSION

Characterization of ABCPs

From Table 2 it is seen that the calculated values of number-average molecular weight $\bar{M}_n$ and NCO group content in prepolymer (I) and (II) are in fairly good accord with the measured values from experiments. This implies that reactions (1) and (2) have finished completely.

The properties of ABCPs made of VTPU based on PPG and styrene monomers (50/50 wt) are shown in *Table 3*. The amount of soluble species varies between 8 and 11%. The analysis of the extract using i.r. spectroscopy shows that absorptions belonging to both polystyrene and PPG phases appear. Excellent damping properties and high adhesive strength between ABCPs and steel imply that ABCPs are excellent damping materials for controlling noise and vibration.

Table 2 Characteristics of prepolymers

	NCO content (%)		$\bar{M}_n$ (g mol^{-1})		
Code	Meas.	Calc.	Meas.	Calc.	η (P) at 25°C
Prepolymer (I)	6.20	6.16	1200	1208	1.26
Preopolymer (II)	0.09	0	1260	1196	12.63
PPG			900		0.0025

Morphology

Figure 1 presents the general morphological features of ABCPs based on VTPU and vinyl monomers such as styrene, vinyl acetate, methyl methacrylate, etc. The dark areas in the micrographs are PU-rich regions, as it is known that OsO_4 preferentially stains the PU component. The composition and characteristics of the prepared ABCPs are summarized in *Table 4*.

All materials display a two-phase morphology, with the plastic component forming the continuous phase and

Table 3 Characteristics of ABCP (VTPU50St50)

Sol fraction (wt%)	11.4
Tensile strength (MPa)	6.2
Tensile modulus (MPa)	8.6
Elongation at break (%)	117
Adhesive strength, with steel (MPa)	9.7
Tan δ_{max}	1.5
Temperature region, tan δ <0.75 (°C)	40

Table 4 Composition and morphological characteristics of ABCPs

	Domain size			
Composition of ABCP	Average (μm)	Range (μm)	$\frac{D_{max}}{D_{min}}$	PU-rich phase content (%)
VTPU50VAc50	0.21	0.70–0.44	6	10.1
VTPU50MMA50	0.50	0.02–0.12	6	14.3
VTPU50St50[a]	0.03	0.02–0.08	4	16.7
VTPU50St50[b]	0.022			

[a] The diameters of domains smaller than 0.02 μm are neglected and $\bar{M}_n$(PPG) = 1570
[b] $\bar{M}_n$(PPG) = 900

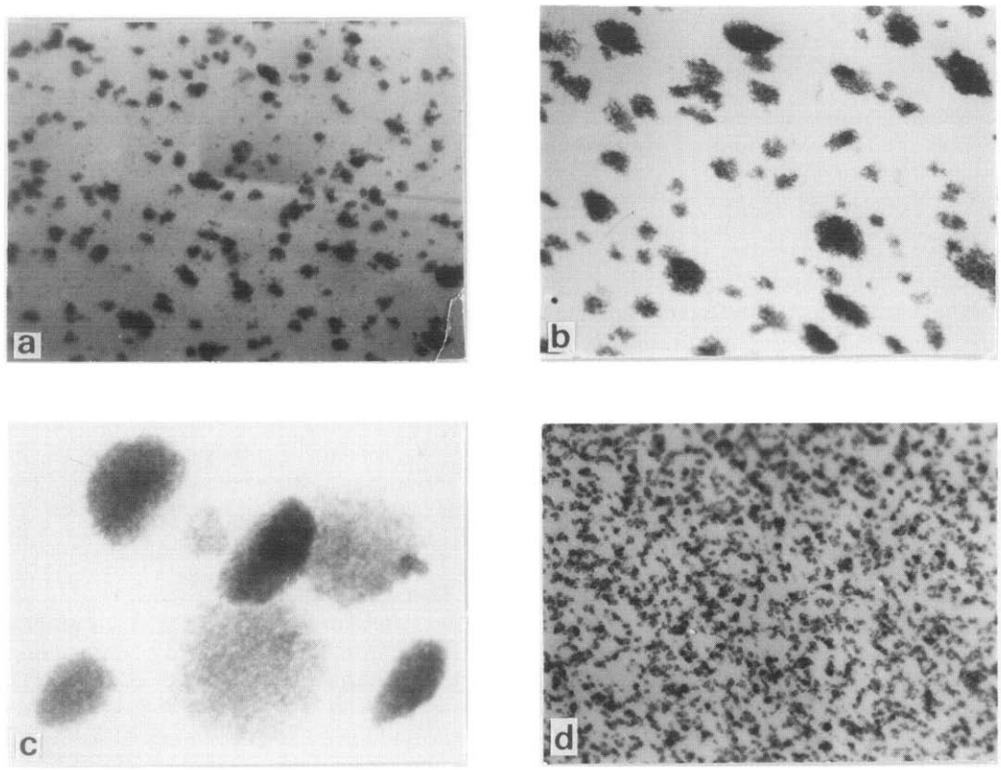

Figure 1 Representative electron micrographs illustrating microphase separation in ABCPs (×50000): (a) VTPU50St50, $\bar{M}_n$(PPG) = 1570; (b) VTPU50MMA50; (c) VTPU50VAc50; (d) VTPU50St50, $\bar{M}_n$(PPG) = 900

the PU-rich domains forming the separated phase. The third column in *Table 4* shows the range of PU-rich domains for three samples. Several differences arise concerning the particle size and their distribution. Column 5 of *Table 4* shows the percentage of PU-rich phase calculated assuming that area fraction is proportional to volume fraction and that the micrographs are representative of the whole samples. These measurements and straightforward observation of the electron micrographs shown in *Figure 1* imply that there is greatest compatibility between the two components in VTPU50St50, and that VTPU50VAc50 has the worst compatibility, having PU-rich domain size 1–2 orders of magnitude larger than those in VTPU50St50 and VTPU50MMA50. This may be due to the difference between the solubility parameters of the two components. Furthermore, a highly polydispere distribution of PU-rich, domain sizes was observed in the three samples, especially in sample VTPU50St50, in which the number of PU-rich domains smaller than 0.005 μm is 3.5 times as great as that of the domains larger than 0.02 μm. However, the volume of these fine domains is only 0.002% of the total volume of PU-rich domains. These results suggest that phase separation occurs at several different times. It appears that this phenomenon is similar to type I and II occlusions observed by Molau and Keskkula[10] in high-impact polystyrene (HIPS) and by Donatelli, Devia *et al.*[11–13] in semi-IPNs and IPNs.

The multi-model distribution of domain sizes in these ABCP systems could possibly arise from phase separation originated by, or a combination of, two processes: (1) multiple precipitation of ABCP chains at different reaction times from VTPU and vinyl monomer mixture; (2) microsyneresis of the networks. Paul[14] has revealed that a completely stable mixture exists for all proportions of the components only when:

$$DM/\rho RT < 2 \tag{4}$$

where D is a binary interaction energy density characteristic of mixing segments of components A and B, and molecular weights M and densities ρ are the same for both components, i.e. $M_A = M_B$ and $\rho_A = \rho_B$. When molecular weight is varied at constant temperature, there will be a range where equation (4) is satisfied and stable, homogeneous mixtures exist for all compositions. At a critical molecular weight M_{cr}, $DM_{cr}/\rho RT$ is exactly equal to 2. Although styrene monomer is compatible with VTPU (i.e. gives clear solutions), polystyrene segments ($M > M_{cr}$) in ABCPs may not be compatible with the mixture of VTPU and styrene, and attempts to prepare such a solution always underwent phase separation.

At the beginning of the polymerization, the free energy of mixing of the system ΔG_m is negative and, therefore, it forms a homogeneous solution. As polymerization proceeds, the molecular weight of ABCP chains increase, ΔG_m becomes positive, primary precipitation of ABCP chains from the mixture solution occurs and the free energy of the system drops to negative values again. On continued polymerization, ΔG_m follows a similar path to secondary and possibly higher-order precipitations. The basis for this mechanism was given by Donatelli *et al.*[12], who observed three ranges of domain sizes in sequential IPNs and derived an equation to predict the maximum size of the domains in sequential semi-IPNs and IPNs. This means that these macromolecules are produced in different environments and so different domain structures appear among them. On the other hand, microsyneresis of the networks with different crosslink densities plays different roles. The syneresis is defined as the contraction of a gel accompanied by the exudation of liquid, and it has been observed by several investigators[15].

The network at the gel point is swollen with styrene and VTPU mixture, and this point represents a maximum in the ability of the network to hold styrene monomer. As the network formation reaction proceeds, the increased crosslink density reduces the network ability to hold the liquid. The concentration of the liquid mixture in excess of equilibrium sweling, the existence of inhomogeneities in the network (such as regions of substantially different crosslink density) and the high viscosity of the mixture solution create favourable conditions for the syneresis process to occur. Phase separation at a microscopic level develops. Free-radical copolymerization itself is able to produce some network with polydispersities in M_c, i.e. crosslink density. The effect increases even more the size differences among PU-rich domains.

Another morphological feature observed in *Figure 1* is that the PU-rich domains all exhibit irregular shapes, which are different from those of some linear block copolymers. For linear AB and ABA block copolymers at equilibrium, only three kinds of morphologies exist, namely spheres or cylinders of the minor component dispersed in a matrix of the major comonent or alternating lamellae of the two components. These structures represent the minimum energy situations attainable for various compositions. In ABCPs, aggregation of the same chains requires the relative movement of network junctions and may be restricted, and the samples exhibit irregular spherical PU-rich domains randomly distributed within the matrix of plastic components. The ABCPs contain more confused morphology of very small domains, and some aggregates of small domains are apparent in the micrographs.

The last column in *Table 4* shows the volume content of the PU-rich domains in ABCPs calculated from the micrographs. The weight percentage of PU generated by TDI in the three samples is 8.1% according to the stoichiometry in ABCP polymerization. Assuming that the weight fraction can be approximately used as a substitute for the volume fraction, it may be inferred from the experimental data that what has been stained is only the segments of PU, though the mechanism for this is still not clear at present.

This point of view can be further supported from the comparison of SEM with TEM micrographs of the samples, shown in *Figures 1* and *2*. In the TEM micrographs the stained PU-rich domains are distributed in the plastic continuous phase, while the SEM micrographs of the same samples give a picture in which the elastometric and plastic components exhibit an alternative arrangement, because the rubber phase in SEM micrographs contains PPG segments.

The calculated content for PU is somewhat lower than values measured from TEM micrographs because the PU-rich domains in the micrographs contain unstained microdomains. The plastic components in PU-rich domains which can be seen from *Figure 1c* had been neglected in the calculated data of *Table 4*. The content of these plastic components in PU-rich domains decreases gradually in the order VTPU50St50, VTPU50MMA50, VTPU50VAc50, as shown in *Table 5*.

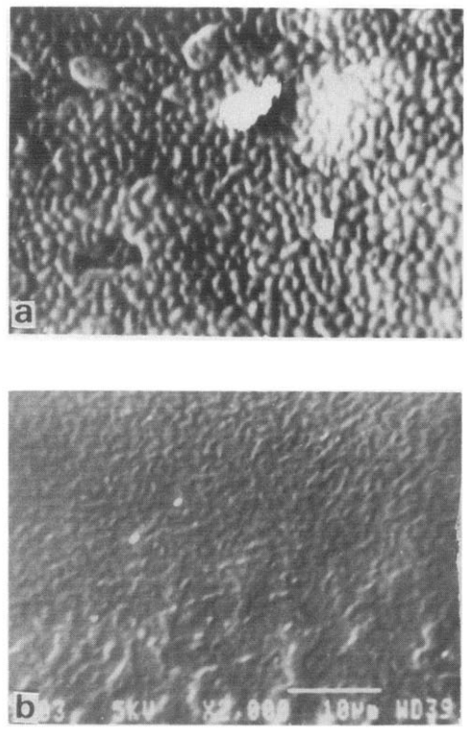

Figure 2 SEM micrographs of ABCPs (× 2000): (a) VTPU50VAc50; (b) VTPU50BMA50

The better the compatibility between the two components in ABCPs, the larger the difference between the observed and calculated percentages of PU-rich domains.

The effect of crosslink density on the domain sizes can be seen from the comparison of (a) with (d) in *Figure 1*. Owing to the change in $\bar{M}_n$ of PPG prepolymer, the increase in crosslink density of the sample will give rise to more fine structures of PU-rich domains.

At high crosslink density, the sol fraction is negligible. The average block length between the junctions will be short and inter-domain separations must be small. This view is consistent with the relatively small PU-rich domains in *Figure 1d*. The most significant differences are the changes in shape of the distributions and the increase in proportion of small domains in VTPU50St50 (d), which reflects a tendency for highly crosslinked structures to produce large numbers of very small domains.

Meier[16] considered the morphologies of AB block copolymers and predicted that the characteristic morphological features would be given by an equation of the type:

$$R = K\alpha C M^{\frac{1}{2}} \tag{5}$$

For spherical domains, R is the domain radius, K is a constant characteristic of the morphology (1.33 for spheres), C is a constant relating unperturbed root-mean-square end-to-end chain dimensions to the molecular weight M of the domain-forming chains and α is a perturbation parameter equal to the ratio of the perturbed to unperturbed chain dimensions. The calculations assumed that the sizes of statistical segments of A and B components were equal, that the chains conformed with random-walk statistics and that the blocks were monodisperse with respect to molecular weight. Following Eastmond[5], the mean diameter of domains $\bar{r}$ in ABCPs can be evaluated by an expression similar to equation (5):

$$\bar{r} = K' \bar{M}_n^{\frac{1}{2}} \tag{6}$$

It was found from the calculation of $\bar{r}$ that the domain size is smaller in ABCPs with the same chemical composition than in AB block copolymers, because A_2BA_2 type ABCPs can be regarded as $A_2B_{\frac{1}{2}}$ copolymers, i.e. B chains behave as if they were half of their true length, reducing the predicted domain diameter by a factor of $2^{\frac{1}{2}}$.

Equation (6) can also be used for the evaluation of the dependence of the size of PU-rich domains in ABCPs on the molecular weight $\bar{M}_n$ of prepolymers. The PU-rich domains $\bar{r}$ are respectively 0.0028 and 0.022 μm on average in ABCPs prepared by copolymerization of styrene with VTPU (50/50 wt) with molecular weight of 1750 and 1260, their ratio (1.27) being close to that of their $(\bar{M}_n)^{\frac{1}{2}}$ (1.17).

The dependence of size of PU-rich domains on the molecular weight of prepolymers can be shown further by (a) and (c) in *Figure 3*. The samples (a) and (c) in *Figure 3* were prepared in a similar way to VTPU50BMA50 except that castor oil (CO) was substituted for PPG. the solubility parameters of COPU and PPGPU are 19.0 and 18.8 $(J\,cm^{-3})^{\frac{1}{2}}$, respectively, the difference between them being very small[17,18]. In contrast, the sizes of PU-rich domains of samples (a) and (c) have an order of magnitude difference. There are more fine structures in castor oil based PU-rich domains, may be due to the fact that the molecular weight for an arm in castor oil is only 601, far smaller than the $\bar{M}_n$ of PPG, so giving rise to a high crosslink density in the sample.

Dynamic mechanical properties

Table 5 shows the compositions and glass transition temperatures of ABCPs and some homo-networks. The tan δ and storage modulus E' vs. temperature curves for the several samples mentioned above are shown in *Figures 4* and *5* respectively. The PU pure elastomer based on PPG shows the lowest glass transition temperature at -35°C and PMMA has the highest T_g at 136°C.

The information from the dynamic mechanical spectra shows that ABCPs based on VTPU and St, MMA and VAc form two-phase polymeric systems. The loss tangent curves in *Figure 4* present two maxima: the upper one, T_{g_2}, is rather pronounced and corresponds to the T_g value of the plastic phase in ABCPs. The lower one, T_{g_1}, is a weak shoulder and its maximum on tan δ *versus* temperature curves cannot be set very accurately. The

Table 5 Composition and T_g values

Code	Composition (wt%)	T_{g_1} (°C)	T_{g_2} (°C)	Solubility parameter $(J\,cm^{-3})^{1/2}$
1	VTPU50MMA50	−15	52	
3	VTPU50BMA50	−31	4	
11	VTPU50St50	−13	56	
13	VTPU50VAc50	−29	13	
	VTPU100	−35		18.8
	COVTPU100	16		19.0
	PMMA100		136	19.0
	PBMA100		68	17.8
	PSt100		128	18.7
	PVAc100		37	19.2

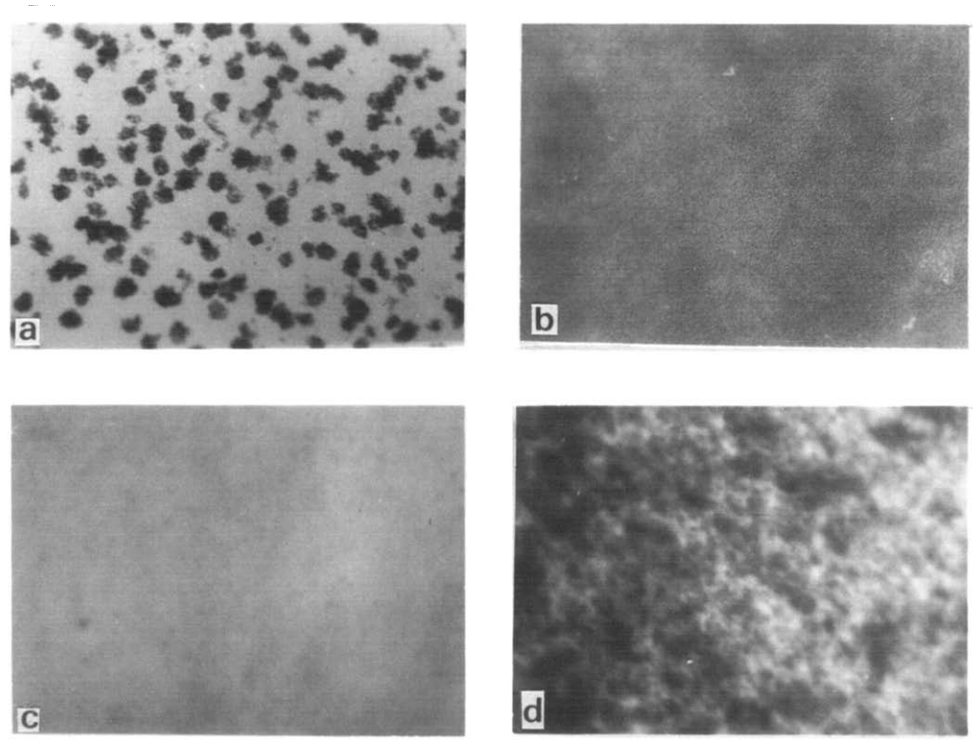

Figure 3 Micrographs of ABCPs: (a) VTPU50BMA50 (× 50 000); (b) COVTPU50St50 (× 50 000); (c) COVTPU50BMA50 (× 100 000); (d) IPN,COPU50/PBMA50 (× 30 000)

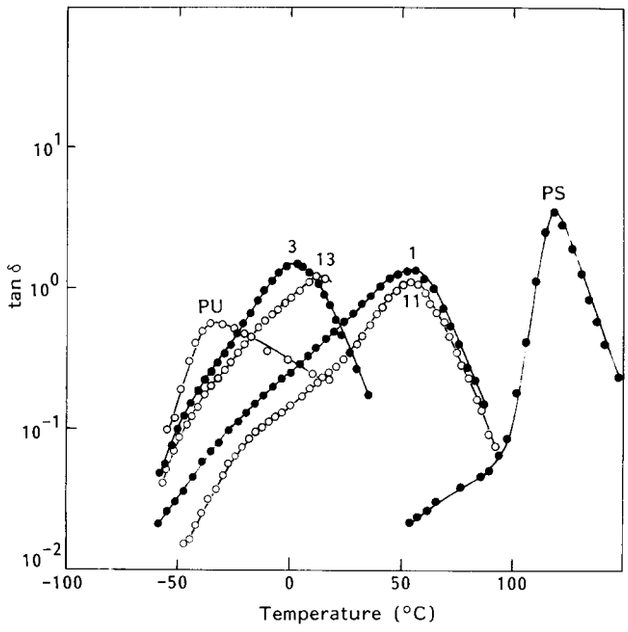

Figure 4 The tan δ vs. temperature plots of ABCPs and homo-networks

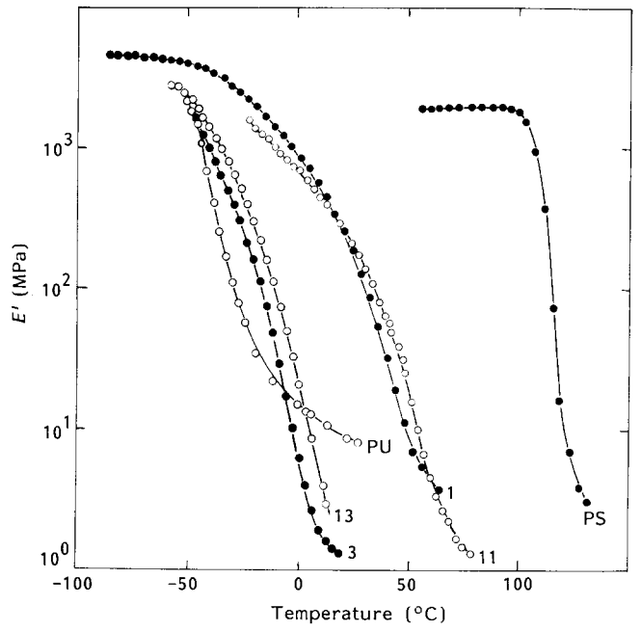

Figure 5 E' vs. temperature plots of ABCPs and some homo-networks

double T_g for these samples evidently have inward shifts compared with T_g values for homo-networks, and this indicates that interpenetration between the two components apparently occurs.

In the E' vs. temperature plots in *Figure 5*, E' of the sample ABCPs have a small drop at T_{g_1} while they have three orders of magnitude drop at T_{g_2}, showing a characteristic of a main transition. The broadening of the glass transition in sample ABCPs is very evident, compared to homogeneous polymer networks. All the observations stated above suggest that there is extensive interpenetration and linking between the two components in ABCPs. The differences in compatibility between the two components are very obvious in the three samples. The compatibility of VTPU50VAc50 is much poorer than that of VTPU50St50 and VTPU50MMA50. The T_{g_1} inward shift is only 6°C against that of PU homogeneous polymer network for the former, while the T_{g_1} inward shift is as high as 22°C for VTPU50St50. This is in accordance with the fact that the size of PU-rich domains

Table 6 An estimate of molecular compositions within each phase

	PU-rich phase		Plastic phase	
Composition	W_1	W_2	W_2	W_1
VTPU50St50	0.79	0.21	0.68	0.32
VTPU50MMA50	0.77	0.23	0.64	0.36
VTPU50VAc50	0.90	0.10	0.72	0.28

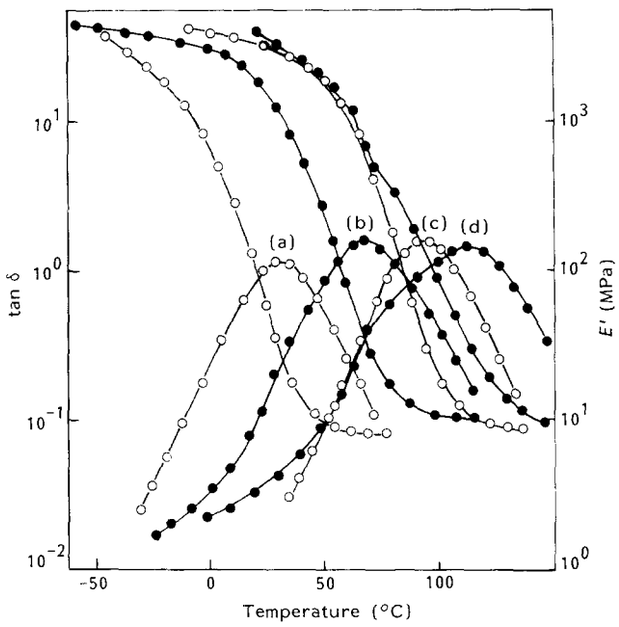

Figure 6 Dynamic mechanical spectra of ABCPs based on COVTPU: (a) COVTPU50BA50; (b) COVTPU50BMA50; (c) COVTPU50St50; (d) COVTPU50MMA50

in VTPU50VAc50 is the largest, as observed in the electron micrographs. If we consider each ABCP to be composed of two isolated phases, one being the PU phase strengthened by plastic, the other the plastic phase plasticized by PU, and the two components are mixed at the molecular level in any phase, the contents for every phase can be calculated according to the Fox equation:

$$\frac{1}{T_g} = \frac{W_1}{T_{g_1}} + \frac{W_2}{T_{g_2}} \tag{7}$$

where $W_1 + W_2 = 1$. The quantity T_g represents the glass transition temperature of the phase in question, and W_1 and W_2 represent the weight fractions of PU and plastic polymer, respectively. The quantities T_{g_1} and T_{g_2} stand for the homo-network T_g vaues. Using the values shown in *Table 5*, the compositions within each phase were calculated and are shown in *Table 6*. The results suggest that 20% St and 80% VTPU mixed at the molecular level in the PU-rich domains. In the St segment the volume fraction of PU based on PPG is about 30%. These results are qualitatively sound although they are not adequate to be treated as quantitative results because many complex factors are not taken into account in the calculation.

These results are consistent with those observed from electron micrographs indicating that there is partial compatibility between the two components. A forced compatibility will develop due to the chemical crosslinking and interlocking of entangled chains that confine the phase separation. In contrast to physical entanglement, a chemical crosslink, cannot be broken.

The dynamic mechanical spectra of ABCPs based on COVTPU are shown in *Figure 6*. The results show that the compatibility between the two components is much better in ABCPs based on COVTPU than in those based on PPGVTPU, because the highest crosslink density has a notable effect on compatibility.

Comparison of the compatibilities of ABCP and IPN

ABCP and IPN samples with similar crosslink densities were selected for the purpose of comparison of compatibility because the crosslink density is a factor that affects compatibility. The dynamic mechanical relaxation spectra for the samples selected are shown in *Figure 7*. It can be seen that the moduli in the rubber state are almost equal to each other for the two samples, and so are the $\bar{M}_c$ values. The composition of the sample ABCP is COVTPU25BMA25(castor oil + TDI)50. In the sample IPN, the castor oil is crosslinked with TDI and BMA with divinylbenzene, and the weight percentages of them both are 50%.

The dynamic mechanical relaxation spectrum of the COPU sample from castor oil crosslinked with TDI is also shown in *Figure 7* for comparison. The IPN sample has very broad double T_g transitions and the superposition of the transitions means an extensive interpenetration of molecular chains. Its T_{g_1} (lower) and T_{g_2} (upper) correspond to the T_g values in the COPU and ABCP samples, respectively. Although the weight percentage of COPU is as much as 75% in ABCP sample, the intensity of relaxation is too weak to be detected at 15°C, which corresponds to the T_{g_1} of IPN, and the tan δ value at 15°C is 0.0175, about half that of the sample IPN at the same temperature. It is not difficult to infer that not only is the compatibility between BMA and COVTPU improved by chemical crosslinking in the sample ABCP, but also the vinyl-terminated castor oil PU (COVTPU) prepolymer can be well dispersed in the

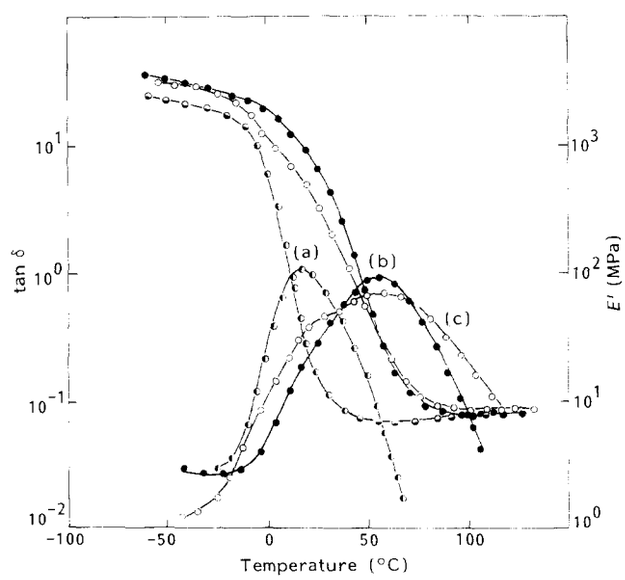

Figure 7 Dynamic mechanical spectra of ABCPs and IPN: (a) COPU (castor oil + TDI); (b) ABCP50(COVTPU25BMA25)/COPU50; (c) IPN, COPU50/PBMA50

COPU (castor oil crosslinked with TDI). Then an improvement in compatibility is achieved. The double T_g values are shown in the Young's modulus E' vs. temperature plot, which corresponds to the tan δ vs. temperature plot. The value of E' decreases by more than three times at T_{g_1} in the IPN sample while no transition or relaxation in the same temperature region was observed in the sample ABCP (COVTPU50BMA50). The E' value in the transition region, between T_{g_1} and T_{g_2}, is obviously higher in ABCP than in IPN, although they have similar E' values in the glass and rubber states, suggesting that there are plenty more isolated rubber phase aggregates in IPN than in ABCP.

Figure 3 shows the electron micrographs of IPN and ABCP (COVTPU50BMA50). The size of PU-rich domains is more than two orders of magnitude larger in IPN than in ABCP, in accordance with the results from the dynamic mechanical analysis. The compatibility of ABCP is better than that of IPN due to chemical crosslinking between two networks in the former.

REFERENCES

1 Sperling, L. H. 'Polymer Blends and Mixtures' (Eds. D. J. Walsh, J. S. Higgins and A. Maconnachie), Martinus Nijhoff, Dordrecht, 1985

2 Bamford, C. H., Eastmond, G. C. and Whittle, D. *Polymer* 1969, **10**, 771, 759, 885

3 Bamford, C. H., Eastmond, G. C. and Whittle, D. *Polymer* 1971, **12**, 247

4 Eastmond, G. C. *Pure Appl. Chem.* 1981, **53**, 657

5 Eastmond, G. C. and Smith, E. G. *Polymer* 1976, **17**, 367

6 Manson, J. A. and Sperling, L. H. 'Polymer Blends and Composites', Plenum, New York, 1976

7 Liu, J. J., Liu, W. Z., Zhou, H. R., Hou, C. R. and Yu, F. S. *Synth. Rubber Ind. (Chin.)* 1986, **9**(4), 266 and 1987, **10**(3), 202; *Chin. J. Appl. Chem.* 1987, **4**(2), 266; *Polym. Mater. Sci. Eng. (Chin.)* 1987, **3**(2), 16

8 Shomoto, K., Ueda, M., Murakami, S., Yamaguchi, H., Minoura, Y., Yamashita, S. and Okamoto, H. *Nippon Gomu Kykaishi* 1977, **50**, 342, 349, 749, 759

9 Kato, K. *J. Polym. Eng. Sci.* 1967, **7**, 38

10 Molau, C. E. and Keskkula, H. *J. Polym. Sci. (A)* 1966, **4**, 1595

11 Donatelli, A. A., Sperling, L. H. and Thomas, D. A. *Macromolecules* 1976, **9**, 671, 676

12 Donatelli, A. A., Sperling, L. H. and Thomas, D. A. *J. Appl. Polym. Sci.* 1977, **21**, 1189

13 Devia, N., Manson, J. A. and Sperling, L. H. *Polym. Eng. Sci.* 1979, **19**(2), 869

14 Paul, D. R. 'Polymer Blends and Mixtures' (Eds. D. J. Walsh, J. S. Higgins and A. Maconnachie), Martinus Nijhoff, Dordrecht, 1985

15 Dusek, K. and Prins, W. *Adv. Polym. Sci.* 1969, **6**, 32

16 Meier, D. J. *J. Polym. Sci. (C)* 1969, **7**, 26 81; *Polym. Prepr.* 1970, **11**, 400

17 Hourston, D. J. and McCluskey, J. A. *J. Appl. Polym. Sci.* 1985, **30**, 2157

18 Devia, N., Manson, J. A. and Sperling, L. H. *Macromolecules* 1979, **12**, 360